EUROFUSION WPJET1-CP(16) 15138

SJP Pamela et al.

Multi-Machine Modelling of ELMs and Pedestal Confinement: From Validation to Prediction

Preprint of Paper to be submitted for publication in
Proceedings of 26th IAEA Fusion Energy Conference

This work has been carried out within the framework of the EUROfusion Consortium and has received funding from the Euratom research and training programme 2014-2018 under grant agreement No 633053. The views and opinions expressed herein do not necessarily reflect those of the European Commission.

Multi-Machine Modelling of ELMs and Pedestal Confinement: From Validation to Prediction

S.Pamela[1], S.Saarelma[1], I.Lupelli[1], C.Maggi[1], C.Roach[1], C.Giroud[1], I.Chapman[1], A.Kirk[1], J.Harrison[1], F.Militello[1], S.Smith[1,2], L.Frassinetti[3], D.Dickinson[2], N.Aiba[4], H.Urano[4], G.Huijsmans[5,6], M.Becoulet[5], T.Eich[7], M.Hoelzl[7], A.Lessig[7], F.Orain[7], S.Futatani[8], SK.Kim[9], OJ.Kwon[10], JW.Ahn[11], F.Liu[12] & JET Contributors[13]

EUROfusion Consortium, JET, Culham Science Centre, Abingdon, OX14 3DB, UK.
1. CCFE, Culham Science Centre, Abingdon, Oxon, OX14 3DB, UK.
2. York Plasma Institute, Department of Physics, University of York, Heslington, York YO10 5DD.
3. Division of Fusion Plasma Physics, KTH Royal Institute of Technology, Stockholm SE.
4. National Institutes for Quantum Radiological Science and Technology, Naka Fusion Institute, Ibaraki 311-0193, Japan
5. CEA, IRFM, F-13108 Saint-Paul-lez-Durance, France.
6. Eindhoven University of Technology, Eindhoven, The Netherlands.
7. Max-Planck-Institut für Plasmaphysik, Boltzmannstrasse 2, D-85748 Garching bei München, Germany.
8. CASE Department, Barcelona Supercomputing Center, Barcelona, Spain.
9. Department of Energy System Engineering, Seoul National University, Korea.
10. Department of Physics, Daegu University, Korea.
11. Oak Ridge National Laboratory, Oak Ridge, TN 37831, USA.
12. ITER Organization, Route de Vinon sur Verdon, 13067 Saint Paul Lez Durance, France.
13. See author list of X. Litaudon, Nuclear Fusion: 26th Fusion Energy Conference, Kyoto, Japan (2016)

Abstract

Future devices like JT-60SA, ITER and DEMO require quantitative predictions of pedestal density and temperature levels, as well as (inter-ELM and ELM) divertor heat fluxes, in order to improve global confinement capabilities while preventing divertor erosion/melting in the planning of future experiments. Such predictions can be obtained from dedicated pedestal models like EPED, and from non-linear MHD codes like JOREK, for which systematic validation against current experiments is necessary. In this paper, we show progress in the validation of the JOREK code using MAST, KSTAR, ASDEX Upgrade, DIII-D, JT-60U and JET simulations, with both qualitative and quantitative comparisons to experiments, and we present the latest achievements of EUROPED as an extension of the EPED model, to clarify the pedestal width description based on kinetic ballooning modes and turbulence. In addition, we describe how JOREK and EUROPED can interact to improve pedestal predictions in cases where ideal MHD fails to describe experimental observations, which is the case for many type-I ELMs in JET-ILW.

1. Introduction

Elaborate experimental scalings for the ITER tungsten divertor provide an estimate of the ELM (Edge-Localised-Mode) and inter-ELM target heat fluxes [1,2]. These predictions can be strengthened by numerical simulations of large-scale instabilities like Peeling-Ballooning (PB) modes to describe the characteristic dynamics of ELMs, as well as small-scale turbulence of Kinetic-Ballooning Modes (KBMs) and Ion-Tempreature-Gradient (ITG) instabilities to describe the cross-field transport in the pedestal which regulates the plasma and energy exhaust across the separatrix in inter-ELM regimes.

Several nonlinear MHD codes, such as JOREK, BOUT++, HESEL and EMEDGE3D in Europe [3-8], M3D-C1 and NIMROD in the US [9,10], or MEGA in Japan [11-13], can obtain advanced ELM simulations, with challenging physics effects like bi-fluid diamagnetic rotation and current, with low resistivity and viscosity level as well as high poloidal/toroidal resolutions. In the last decade, nonlinear MHD codes have focused their efforts on obtaining qualitative agreement with experimental observations, by considering key ELM characteristics like the formation of hot plasma filaments that are ejected through the separatrix, the collapse of the pedestal pressure, and the transport of energy to the divertor and first wall components.

The implicit scheme used by the JOREK code to evolve the peeling-ballooning dynamics involves solving large sparse matrices systems, therefore bringing the computational requirements of such nonlinear MHD simulations to a level close to that of large kinetic simulations with explicit schemes. Nevertheless, recent increases in computational resources available to fusion research are now enabling the start of quantitative comparisons with experiments, which is the compulsory path towards predictions for future devices like ITER. In sight of the urgent need for such predictions, this paper discusses the latest progress of mutli-machine qualitative and quantitative validations for the nonlinear MHD code JOREK.

In addition to the peeling-ballooning instabilities used to describe ELMs, small-scale turbulence simulations are needed for the inter-ELM regime. This is required not only for the evaluation of inter-ELM divertor heat-fluxes, but also for the prediction of pre-ELM pedestal pressure levels, which is determined broadly by how the pedestal profiles evolve until the ELM onset (determined by MHD stability). Turbulence codes like GS2 and ORB5 [14,15] can evaluate the stability of KBMs in the pedestal, which are believed to regulate the pedestal pressure gradient during the inter-ELM phase [16,17]. Although nonlinear MHD codes can evolve the inter-ELM pedestal profiles using ad-hoc assumptions (eg. fixed gradient or fixed width), in order to obtain reliable predictions for future devices, a coherent picture including turbulence is necessary.

Both the inter-ELM pedestal evolution and the ELM crash share a common feature, the H-mode transport barrier. Significant progress has been achieved in recent years by nonlinear codes like HESEL, EMEDGE3D or CENTORI [7,8,18], and one of the main challenges of inter-ELM and ELM simulations at present is to determine whether a coherent description of the H-mode transport barrier is required to obtain realistic and accurate evaluations of modes stability in the pedestal (both turbulence and PB modes). In this paper, we will address this important issue with respect to JOREK simulations.

The paper is organised as follows. In Section-2, we present the current state of JOREK simulations on multiple devices, such as MAST, ASDEX Upgrade, KSTAR, JT-60U and DIIID, including recent progress in qualitative agreements with the experimental observations. In Section-3, we describe recent advances in the quantitative validation of JOREK simulations for ELMs in JET with multiple discharges, and discuss the challenging issue of unexplained pedestal stability for high-gas ILW discharges. In Section-4, we present the latest results of EUROPED concerning pedestal turbulence in the inter-ELM phase, and explain how JOREK can be used within EUROPED to improve ideal MHD predictions of the ELM stability. In the conclusion, Section-6, we discuss how predictions for future devices with the JOREK code need to rely on multi-cylce ELM simulations, and what this implies for future simulations.

2. JOREK simulations of ELMs for multiple devices

In recent years, JOREK simulations have been adapted to various tokamak devices, with the aim of achieving a multi-device validation of the JOREK code. KSTAR simulations have been run to compare the filament rotation with the 2DECE diagnostic. The same rotation frequency is obtained by JOREK, with filaments rotating inside the pedestal before being ejected across the separatrix [19]. DIII-D simulations of ELMs were performed to study the relation between mode numbers and X-point lobes, including divertor heat-flux patterns. JT-60U simulations have been started and comparison with the linear MHD code MINERVA [20] is underway. Figure-1 shows poloidal cross sections of these 4 devices during an ELM crash.

ELM simulations based on ASDEX Upgrade equilibria have shown the development of poloidally and toroidally localized structures [21] and the excitation of low mode numbers by non-linear mode coupling at low resistivity and viscosity [22]. In the non-linear phase, a broad mode-spectrum develops and filament dynamics as well as energy losses are comparable to experimental observations [23]. Divertor footprints and the asymmetry between high and low field sides [24] as well as the ELM control via RMP fields [25] and pellets [26] are studied.

Improved simulations for MAST have been obtained to demonstrate the ability of JOREK to reproduce isolated filaments. In particular, comparisons with the fast visible camera, first attempted in [27], showed that the highest mode number was creating a crash without nonlinear coupling with lower modes. In more recent simulations, using lower resistivity and viscosity, and including diamagnetic effects, nonlinear coupling between modes is obtained. This results in isolated filaments of various sizes at the edge of the plasma, which can be compared to experimental observations, as shown in Figure-2. In particular, complex filament dynamics are observed in these simulations, where filaments inside the separatrix rotate poloidally towards each other, until they merge, at which point the resulting single filament is expelled across the separatrix. Further improvements will be sought in the future to reproduce the dynamics of these filaments in the SOL, where they slow down after crossing the separatrix (in the experiments they travel at increasing speeds in the far SOL [28]). It is yet not clear whether SOL conditions in simulations are responsible for this difference, or if boundary conditions for the current on the divertor targets could be important, as they have been predicted to play a major role in upstream filament dynamics [29].

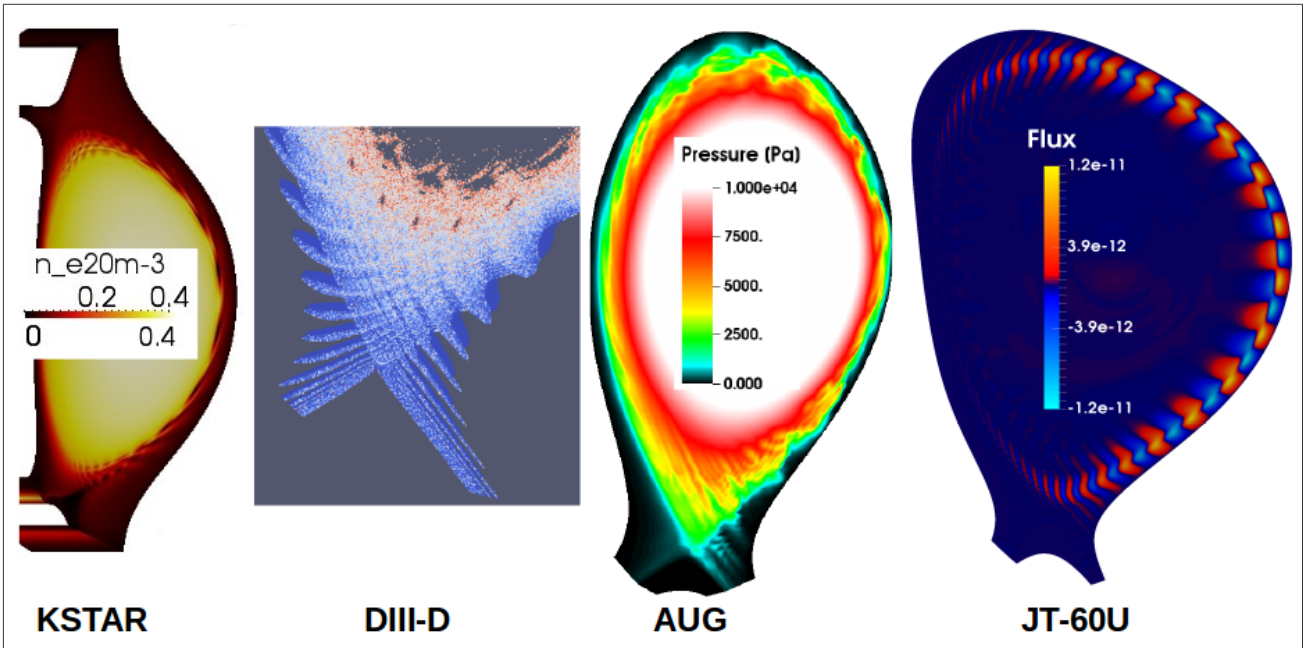

Figure-1:
ELM simulations of KSTAR, DIII-D, ASDEX Upgrade and JT-60U. The validation of JOREK against multiple tokamak devices needs to be adapted depending on the availability of diagnostics for each device. The KSTAR case shows density filaments rotating at the edge of the plasma. The DIII-D case shows a Poincaré plot of perturbed field lines in the vicinity of the separatrix, where the pedestal region is strongly ergodized, and lobe structures are observed along the X-point. The ASDEX Upgrade case shows pressure filaments during an ELM, where toroidal mode coupling results in fragmented filaments. The JT-60U case shows the perturbation of the poloidal magnetic flux during an ELM.

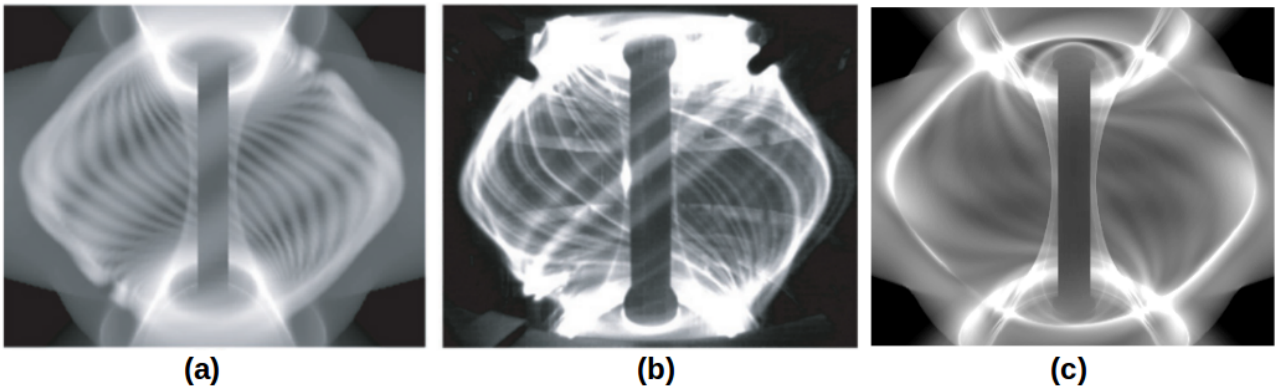

Figure-2:
Fast camera images of MAST simulations. (a) pictures a simulation where the mode n=20 is entirely dominant over all other modes. (b) shows a fast visible camera image of an ELM during a MAST discharge, where multiple mode numbers are coupled. (c) pictures a simulation where coupling between lower and higher modes results in large filaments isolated amidst other smaller filaments in the background.

3. Quantitative simulations of JET

The 3D nonlinear MHD code JOREK was initially developed with the aim of producing ELM simulations [3,4]. The MHD model used here is described in previous ELM studies [30]. It is a reduced MHD model which evolves the five variables ψ (poloidal magnetic flux), Φ (electric potential), $v_{//}$ (parallel velocity), ρ (mass density), T (temperature), including diamagnetic effects.

The pulses used for the simulations are the same JET-ILW as in [30]. In this previous work, the total energy losses were reproduced by the simulations, but the divertor heatfluxes were significantly lower than in the experiments. The simulated ELMs were less intense, but lasted longer than in the experiments (which is why the total energy losses were comparable). In this recent work, those simulations were improved in several ways.

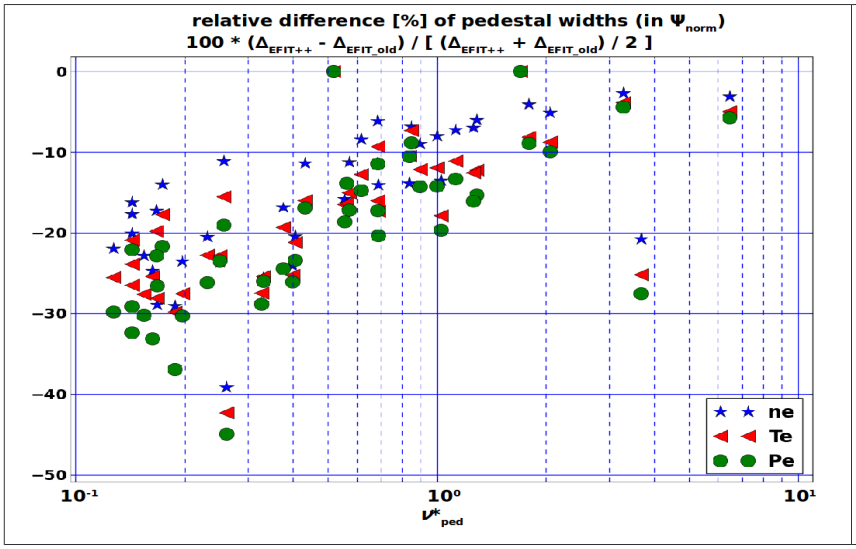

Figure-3:
The pressure, polarimetry and MSE constraints in EFIT, together with allowing for pedestal current in the equilibrium reconstruction, have a strong effect on the mapping of the n_e and T_e profiles from the HRTS diagnostic. The left plot shows the difference, in %, between standard EFIT and EFIT++, for the pedestal width of the ne, Te and pe profiles. The ψ-mapped pedestal width can be >30% smaller with EFIT++.

The first improvement brought to the simulations concerns the magnetic equilibria used to map the n_e and T_e profiles. In [30], the standard EFIT equilibria were used, with magnetic constraints only, whereas additional constraints (pressure, polarimetry, motional stark effect MSE) in recent versions of EFIT++/JEC2020 [31] were used for the new simulations. The most important difference between the two versions of EFIT (with respect to ELM simulations) is that the latter version allows for pedestal currents. This modifies the magnetic flux gradient in the pedestal region, such that when the High-Resolution Thomson Scattering (HRTS) n_e and T_e profiles are mapped from real space onto the magnetic equilibrium, the resulting pedestal gradient width (in ψ-space) is modified. For these pulses it is found, as shown in Figure-3, that the gradient width can be diminished as much as 40% for low collisionality pulses (ie. those with the largest pedestal current). This effect was expected to have a strong influence on the discrepancy obtained in the first study of [30]. The second improvement of the simulations, is that full diamagnetic effects are used for the simulations, as well as multiple toroidal mode numbers, which was not the case in the previous study. The new simulations were run with toroidal mode numbers n = 3, 6, 9, 12, 15. All simulations were run with a resistivity level at a factor 10 above the Spitzer resistivity, which depends on the absolute temperature profile of each pulse. The viscosity level is 4.10^{-8} $kg.m^{-1}.s^{-1}$ for all pulses. The parallel conductivity, which also depends on the absolute temperature for each pulse, was taken between the ion and the electron Braginskii coefficient, at a factor 4 above the ion Braginskii value. The difference between these various MHD parameters and the experimental values (where available) results from current numerical limitations for the simulations. In particular, obtaining simulations at low resistivity with full diamagnetic effects is numerically challenging due to strong diamagnetic currents obtained during the ELM crash.

Although the divertor heat-flux is similar, for most pulses, to the previous simulations of [30], the total ELM energy losses are much lower due to the stabilizing effect of the diamagnetic terms, which diminishes the time duration of the ELM crashes. This is shown in Figure-4, where the new simulation results are plotted together with the previous results from [30].

Nevertheless, some cases are relatively well reproduced, both in terms of divertor heat flux, as well as energy losses. In particular, low-gas pulses like 83330 and 83334 are in good agreement with the experiments. Using these two cases, a collisionality scan was performed by varying the density level at constant pressure. The result is also in good agreement with the experiments, as shown in Figure-5. High-gas experiments are usually not well reproduced by JOREK, since the pressure profiles are well inside the stable region of peeling-ballooning modes, as is regularly observed for ILW high-gas pulses [32,33]. In particular, the T_e pedestal profile is further inside the separatrix than the low-gas pulses, which has a considerable effect on the PB-stability.

The ν^* scans shown in Figure-5 demonstrate two important aspects of the JOREK simulations. First, provided the pre-ELM pressure profiles are above the MHD stability threshold, the simulations are able to reproduce the ν^* dependency of the parallel energy transport from the pedestal to the divertor. Secondly, since energy exhaust is reproduced for these low-gas cases, it means that for high-gas cases, either some physics ingredient is missing, or the pre-ELM profiles taken from HRTS are not

representative of the total pressure profiles including for ion temperature at the very edge of the pedestal. Additional physics effects could be required in JOREK to enable agreement with high-gas experiments, like the neutrals model [34,35], or the effect of tungsten impurities [36], or possibly some other mechanism that may be responsible for triggering an ELM where standard MHD models say there shouldn't be any.

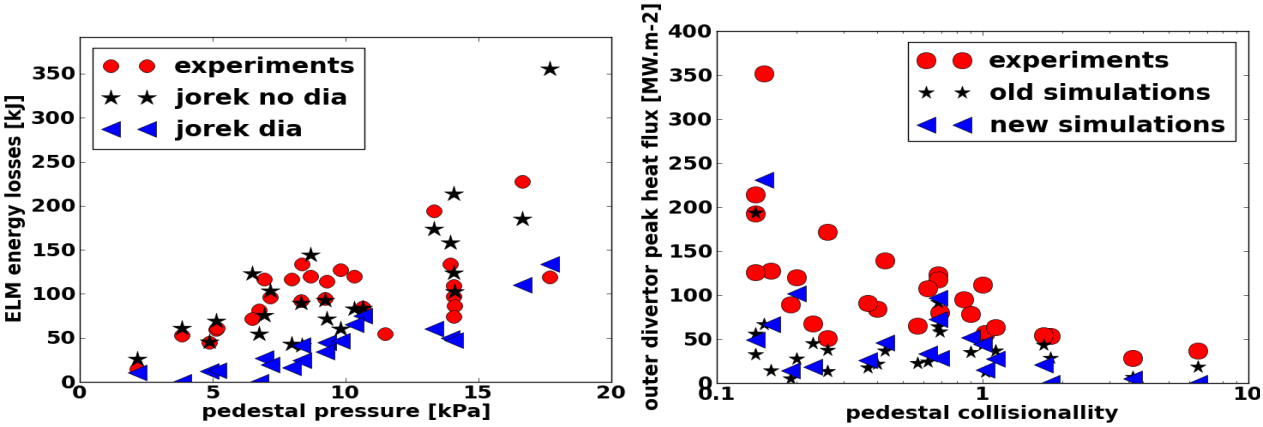

Figure-4:
Quantitative comparisons of ELM simulations with JOREK against experiments. The left plot shows the ELM energy losses as a function of pedestal pressure. The right plot shows the divertor peak heat flux (during the ELM) as a function of the pedestal collisionality ν^*_{ped}. The red circles are the experimental values, measured by HRTS (left), and by IR-camera (right), with one point per discharge (averaged over all ELMs). The black stars are the old simulations performed in [Pamela2015]. The blue triangles are the new simulations, performed with improved equilibrium reconstructions (EFIT++), with diamagnetic terms and with multiple toroidal harmonics. Note simulations are shown as one point (one simulation) per discharge.

One of the most important aspects of simulations is the occurrence (and non-occurence) of nonlinear mode coupling during the ELM crash. In most cases, a dominant mode number leads to the crash, while minor coupling with the other modes occurs only at the end of the ELM, once most of the energy has already been evacuated. In a few cases, the coupling occurs earlier in the crash, but there is usually still one dominant mode number. However, if the pedestal pressure is restored using density fueling and heating, strong nonlinear coupling can be obtained after the first crash. An example of such behaviour is shown in Figure-6, where a small ELM crash is obtained without any nonlinear coupling, and following this crash, with additional heating and fueling, a second large ELM crash is obtained. Note that the simulation is started with a low pedestal pressure, not with the pre-ELM profiles, so that the first crash, at –0.7*ms*, is not one of the cases in Figure-4 and Figure-5.

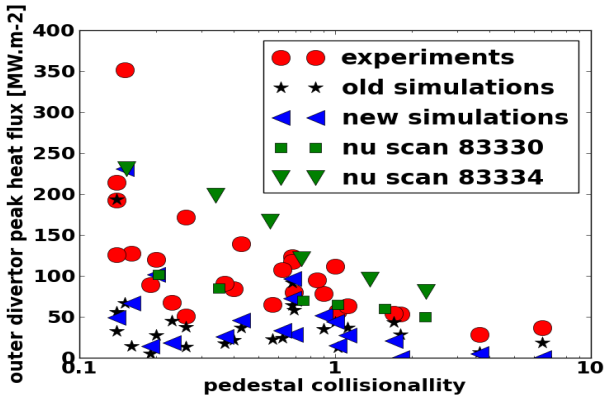

Figure-5:
Simulations of v scans for pulses 83330 and 83334 give a good agreement with experimental data, which demonstrates that JOREK can describe the parallel energy transport, provided the initial pedestal stability before the ELM, is coherent (ie. unstable). The green v* scan for each pulse is done by varying the amplitudes of the n_e and T_e profiles at constant pressure.*

Given Figure-6, it would be natural to attempt to use the same method for all pulses in order to obtain larger ELM crashes that would improve the comparisons in Figure-4. However, this is not straight forward, and there are fundamental issues with this approach. The first issue is that this second ELM has a heat-flux almost twice higher than in the corresponding experiment, and a total energy loss 3 times higher. The other issue is that it is not trivial to reconstruct the pedestal in an experimentally relevant manner. For this case, the width of the pedestal was kept constant, and only the pedestal height was increased, which is numerically the easier option, but the pre-ELM pedestal pressure, at –0.1*ms*, is about 10% higher than the experimental value. Therefore, there is no guarantee that the pre-ELM

profiles will be coherent with the corresponding experimental case. In addition, there is no guarantee that this method will be successful for all cases. In fact, Figure-6 is based on pulse 83334, which is initially a good case, and therefore, it is normal that when recovering the pedestal pressure, a large ELM is obtained. But for other cases, where the experimental pre-ELM profiles are stable, it might be necessary to increase p_{ped} much further before such a large ELM is obtained (if the position of the n_e and T_e pedestals are not modified during the pedestal recovery). Finally, such simulations are numerically expensive, due to the high level of mode activity, which requires times steps of the order of $0.05\mu s$ in the most nonlinear phase of the crash.

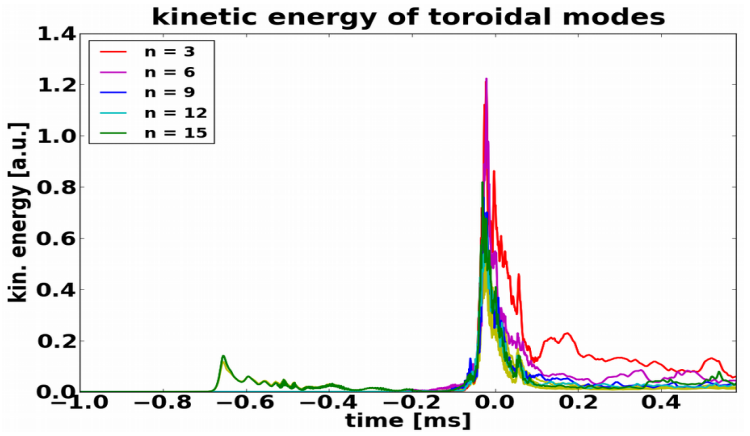

Figure-6:
Simulation of an ELM with nonlinear coupling between toroidal modes. The simulation is started with a stable pedestal pressure gradient, and the ne and Te profiles are progressively recovered using a density and temperature source. A first small crash is observed, at -0.7ms, where no coupling between modes occurs, but when the pedestal pressure is further increased, a large ELM crash is eventually obtained, with strong coupling between toroidal modes.

Eventually, the complete validation of the JOREK code will require its ability to predict pre-ELM profiles for such cases, in agreement with experiments, and although this could be achieved for a single pulse, to obtain quantitative agreement for several pulses will be a major challenge, and will require significantly more numerical resources. In any case, such studies, together with the exploration of multi-cycle ELM simulations and inter-ELM profiles evolution, will require some additional input which JOREK cannot provide self-consistently at present: the small-scale turbulence in the pedestal which regulates the pressure gradients.

4. Inter-ELM pedestal stability with EUROPED

The EPED model provides an estimate of pre-ELM pedestal pressure by combining an n=∞ KBM (Kinetic Ballooning Modes) constraint and an ideal PB (Peeling-Ballooning modes) constraint on the pedestal. However it is not certain whether KBMs, or other microinstabilities, are the turbulent modes that regulate the pressure gradient in the experiments.

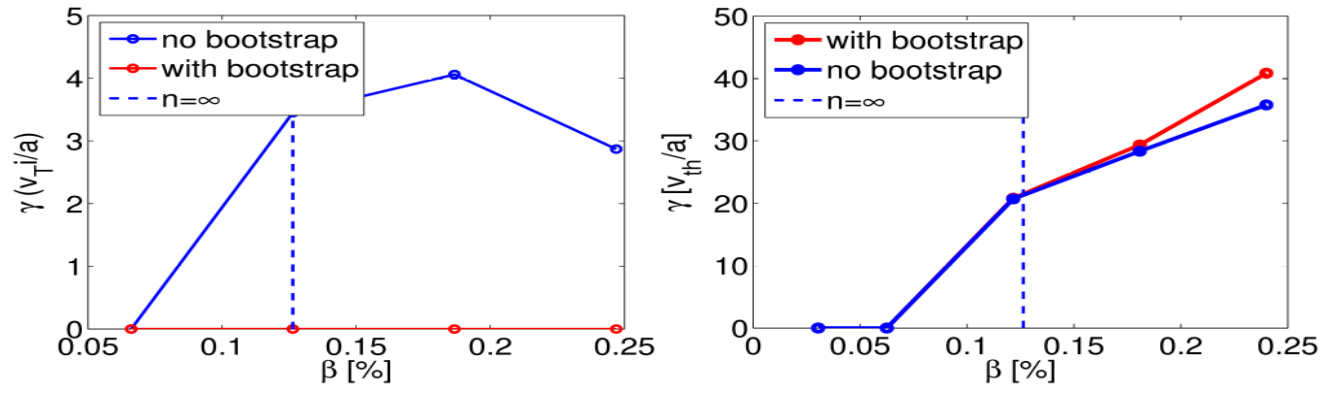

Figure-7:
The local (left) and global (right) KBM growth rates at the most unstable pedestal location as a function of β with (red) and without (blue) bootstrap current taken into account in the equilibrium reconstruction. The dashed line shows the n=infinity ballooning mode boundary.

The global electromagnetic gyrokinetic analysis found that the access to 2nd stability for KBMs present in the local gyrokinetic and ideal MHD analysis in the pedestal region with high bootstrap current is closed by the global effects. In both JET and MAST pedestals the global β limit for the KBMs is found to agree with the local β limit that corresponds to the equilibrium reconstructed without

the bootstrap current. While the local analysis found KBMs stabilised by the inclusion of bootstrap current into the equilibrium it had no effect on the global KBM stability limits, as shown in Figure-7.

For predictive pedestal models constructed using local stability criteria to constrain the pedestal gradients, the global result indicates that the 2nd stability access for KBMs does not exist when the non-local effects are taken into account and the local limit constructed based on an equilibrium without the 2nd stability access for KBMs. It is still unclear why the global result disagrees with the local at low magnetic shear, and this will be the focus of the future work.

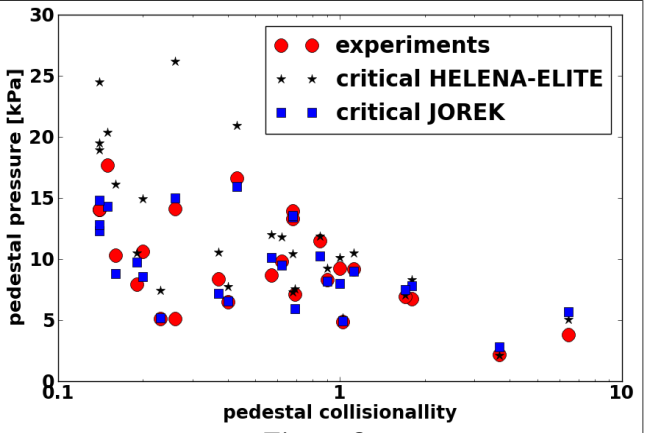

Figure-8:
The ELM-stability predicted by JOREK can be used to improve EUROPED calculations for JET-ILW experiments. The red circles show the experimental pre-ELM p_{ped} levels. The black stars show the ideal MHD critical p_{ped} levels calculated for finite-n PB-modes with ELITE and HELENA (for the equilibrium). The blue squares show the critical p_{ped} levels calculated by non-ideal MHD with JOREK.

Such KBM models could, in the future, prescribe input constraints for JOREK simulations when reconstructing the inter-ELM pedestal profiles. On the other hand, JOREK simulations can also be used to improve EUROPED predictions. The ELM onset criterion used by EUROPED relies on ideal linear MHD for the peeling-ballooning modes. However, this fails for many JET-ILW cases, as the experimental pre-ELM profiles are observed to be far inside the stable region of the j-α diagrams. JOREK, which uses a visco-resistive MHD model, can be used to predict the ELM onset by running simulations as shown in Figure-6. Although it is yet not understood how JOREK can predict the linear MHD threshold without reproducing the correct ELM energy losses, the agreement with the experiment is not negligible, as shown in Figure-8, particularly at low pedestal collisionality. In Figure-8, the critical ideal MHD limit is determined by calculating many HELENA equilibria with increasing p_{ped} values (and self-consistent bootstrap current) until the ELITE [37,38] calculations for finite-n PB-modes show that the stability threshold has been crossed. The critical non-ideal MHD limit is determined by running JOREK, starting from a stable p_{ped} value, and increasing it progressively until a mode becomes unstable (ie. like at -0.7ms in Figure-6).

5. Conclusion: implications for future predictions

The interaction between nonlinear MHD and inter-ELM predictive models like EUROPED is, at present, unavoidable. There are two major issues with multiple-ELM simulations, for JOREK and more generally, for any nonlinear MHD model. The first one is that the inter-ELM profiles need to be evolved rigorously, following some rules set by other transport models, like small-scale turbulence which regulates the pedestal pressure gradients in the inter-ELM phase. However, this can be challenging for numerical reasons as well as physical reasons. To evolve the pedestal with a constant width is straight forward, but as shown above, the ELM onset might not necessarily occur at the same pedestal top pressure as in the experiments, which makes the validation against those experiments impossible. Using a fixed gradient as constraint can be even more difficult, simply because peeling-ballooning modes remain active in the inter-ELM phase of the simulations. This is the second issue, namely that even if the MHD modes do not evacuate much energy in the inter-ELM phase, they still have a non-negligible effect on the pedestal profiles. In addition, the transition between this intermediate state and the ELM crash is not understood at this point. From present simulations, it seems clear that in order to obtain a large type-I ELM crash, the pre-ELM activity of the modes must be as low as possible. A good example of this is the simulations performed by M.Becoulet and EMEDGE3D, where the inter-ELM state of the modes is stabilised by means of an increased sheared pedestal flow [19,39,8]. However, this now raises an important question for all ELM simulations obtained by nonlinear MHD codes: namely, whether multiple type-I ELM cycles can or cannot be modelled without first modelling a coherent background H-mode transport barrier, as done by the HESEL simulations [7].

It must be noted that in the multiple ELM cycle simulations presented in Figure-9, the resistivity is still a factor 7 from the realistic Spitzer value, which is known to have a strong effect on ballooning mode stability. Nevertheless, there is no guarantee that lowering resistivity further (which would be numerically more challenging) would stabilize the modes in the inter-ELM phase.

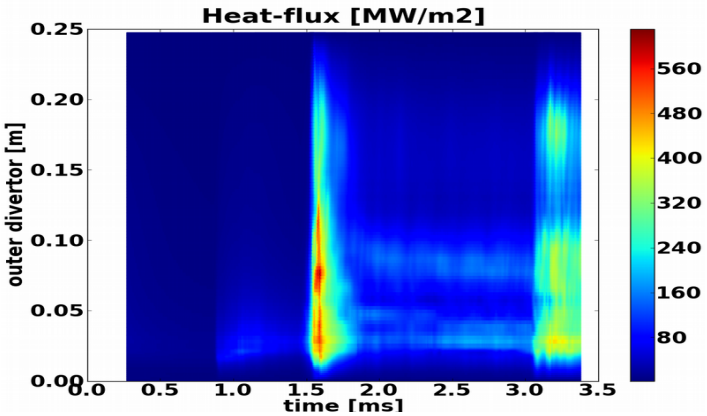

Figure-9:
Simulation of the inter-ELM phase and a second ELM starting from the simulation presented in Figure-6. The x-axis represents the time evolution, the y-axis the outer divertor, and the color scaling the divertor heat-flux.

Most importantly, at this point it is crucial to acknowledge that the present results obtained here are strongly suggesting that ELM simulations with JOREK cannot be validated on current machines using pre-ELM pedestal profiles, and any prediction for future devices must rely on a validation done with multiple-ELM cycles. This, in any case, should be the next focus of JOREK simulations, since for future devices, we do not know what the pre-ELM pedestal profiles will be, such that the ELM predictions must include the prediction of the pre-ELM pedestal profiles as well. In this context, the necessity of solving the H-mode transport barrier coherently (and therefore small-scale turbulence), in order to obtain multiple ELM cycles, becomes a major question.

Acknowledgements

This work has been carried out within the framework of the EUROfusion Consortium and has received funding from the Euratom research and training programme 2014-2018 under grant agreement No 633053, and from the RCUK Energy Programme [grant number EP/I501045]. To obtain further information on the data and models underlying this paper please contact PublicationsManager@ccfe.ac.uk. A part of this work was carried out using the HELIOS supercomputer system (IFERC-CSC), Aomori, Japan, under the Broader Approach collaboration, implemented by Fusion for Energy and JAEA. The views and opinions expressed herein do not necessarily reflect those of the European Commission or the ITER Organization. A part of this work used the HEC ARCHER computer in UK as part of the Plasma HEC Consortium EPSRC grant number EP/L000237/1. A part of this work used the MARCONI computer at CINECA in Italy.

References

[1] T. Eich *et al.*, J. of Nucl. Mat. 390-391 (2009)
[2] T. Eich *et al.*, Nucl. Fusion **53** (2013)
[3] G. Huysmans et al., Nucl. Fusion **47** (2007)
[4] O. Czarny et al., J. Comp. Phys. **227** (2008)
[5] G. Huijsmans et al., Nucl. Fusion **53** (2013)
[6] B.Dudson et al., J. of Plasma Phys. **81** (2014)
[7] A.Nielsen et al., Phys. Letter A **379** (2015)
[8] G. Fuhr et al. , Phys. Rev. Lett. **101** (2008)
[9] S.Jardin et al., Phys. Plasmas **12** (2005)
[10] C.R. Sovinec et al., J. of Comp. Phys. **195** (2004)
[11] Y. Todo et al., Phys. Plasmas 12 (2005)
[12] Y. Todo, Phys. Plasmas 13 (2006)
[13] Khan R et al., Phys. Plasmas **14** (2007)
[14] M.Kotschenreuther, Comp. Phys. Commun. **88** (1995)
[15] S.Jolliet et al, Comp. Phys. Commun. **177** (2007)
[16] S.Saarelma et al., Varenna Conf. Proceedings (2016)
[17] P.Snyder et al., Nucl. Fusion **51** (2011)
[18] A.Thyagaraja et al, Phys. Plasmas **17** (2010)
[19] M.Becoulet et al., 26th IAEA Conf., Kyoto (2016)
[20] N.Aiba et al., Comp. Phys. Commun. **180** (2009)
[21] M.Hoelzl et al., Phys. of Plasmas, **19** (2012)
[22] I.Krebs et al., Phys. Plasmas **20** (2013)
[23] F.Orain et al., 43rd EPS Conf., Leuven, P1.17 (2016)
[24] A. Lessig et al, Phys. of Plasmas (in preparation)
[25] F.Orain et al., 26th IAEA Conf., Kyoto (2016)
[26] S.Futatani et al., 26th IAEA Conf., Kyoto (2016)
[27] S. Pamela *et al.*, Pl. Phys. Control. Fus. **55** (2013)
[28] A.Kirk et al., Pl. Phys. Control. Fus. **48** (2006)
[29] T.Evans et al., J. of Nucl. Mat. **390** (2009)
[30] S. Pamela *et al.*, Pl. Phys. Control. Fus. **58** (2015)
[31] L.Appel et al., 33rd EPS Conf., Rome, P2-184 (2006)
[32] C.Maggi et al., Nucl. Fusion 55 (2015)
[33] C.Giroud et al., 26th IAEA Conf., Kyoto (2016)
[34] A.Fil et al., Phys. Plasmas **22** (2015)
[35] M.Verbeek et al., 43rd EPS Conf., Leuven, P5.58 (2016)
[36] D.VanVugt et al., 43rd EPS Conf., Leuven, P5.57 (2016)
[37] H.Wilson et al., Phys. Plasmas **9** (2002)
[38] P.Snyder et al., Phys. Plasmas **9** (2002)
[39] F.Orain et al., Phys. Rev. Lett. **114** (2015)